processes

MDPI

Article

Study on Erosion Wear of Single- and Double-Orifice Throttling Tools for Underground Coal Gasification

Jianjun Wang [1,2,*], Bingchao Zhou [1,2], Jianglong Fu [3], Siqi Yang [2], Chao Wang [3] and Xiangyi Ren [2]

[1] State Key Laboratory of Performance and Structural Safety for Petroleum Tubular Goods and Equipment Materials, CNPC Tubular Goods Research Institute, Xi'an 710077, China; zhou_bingchao@163.com
[2] Mechanical Engineering College, Xi'an Shiyou University, Xi'an 710065, China; yangsiqi@cnpc.com.cn (S.Y.); renxiangyi@cnpc.com.cn (X.R.)
[3] The Second Gas Plant of PetroChina Changqing Oilfield Company, Yulin 719000, China; fujl01_cq@petrochina.com.cn (J.F.); wchao_cq@petrochina.com.cn (C.W.)
* Correspondence: wangjianjun005@cnpc.com.cn

Abstract: In underground coal gasification, as a choke regulating the formation gas lift pressure, the throttling tool can effectively reduce the production cost, the number of ground heating and insertion equipment, and gas consumption. Because in this process, the coal is transformed into composite synthetic gas through a series of technical treatments, the throttling tool is in a working environment with high temperature and pressure. In the process of transportation of combined synthetic gas, the pulverized coal parts produced by incomplete coal combination move with the gas in the throttling tool. The high temperature and high-pressure gas carrying large-diameter pressed coal parts will cause serial erosion and wear to the throttling device, resulting in failure and well-controlled safety risks. Therefore, according to the Joule–Thomson effect, this paper independently designs downhole throttling tools with single- and double-hole structures. According to actual field conditions, the erosion wear of throttling tools with different systems in high-temperature gas–solid two-phase flow was simulated and predicted, and the internal flow field characteristics of throttling means were analyzed. The difference between the wall wear distribution, wall collision position, and wall erosion effect of different structure throttling mechanisms with the change in gas velocity was investigated, which guides the practical use of the subsequent throttling tools.

Keywords: underground coal gasification; erosion; throttling tool; numeral simulation; high temperature

Citation: Wang, J.; Zhou, B.; Fu, J.; Yang, S.; Wang, C.; Ren, X. Study on Erosion Wear of Single- and Double-Orifice Throttling Tools for Underground Coal Gasification. *Processes* **2024**, *12*, 120. https://doi.org/10.3390/pr12010120

Academic Editors: Hsin Chu and Raymond Cecil Everson

Received: 31 October 2023
Revised: 4 December 2023
Accepted: 15 December 2023
Published: 2 January 2024

1. Introduction

Underground coal gasification (UCG) is a complex process as it depends on many factors such as geological and geo-hydrological analysis of strata, physical and chemical properties of coal, operational process parameters, seismic events, and analysis of produced gases in real time [1]. Changing the general approach to mining methane as an alternative and more environmentally neutral energy carrier (than coal) implies that gassy coal deposits should be perceived as sources of unconventional coal gas collectors (due to technogenically disturbed rock massifs). The use of electricity and heat obtained from the cogeneration (trigeneration) of the extracted gas for the internal consumption of the mine allows for a synergistic effect of reducing the cost of coal mining and the sale of futures to reduce CO_2 emission units and increase the safety of mining [2]. In the process of UCG, as a choke regulating formation gas lift pressure, the throttling tool can effectively reduce the production cost, the number of ground heating and insulation equipment, and the gas consumption. However, in the process of underground coal gasification mining, the throttling tool is in a high-temperature and high-pressure working environment, and the solid particles entrained in the mined crude gas collide with the pipe string, causing varying degrees of erosion and wear on the pipe string wall. So, the downhole throttling tools with

double throttling holes still face the erosion wear of throttling tools caused by solid particles, and the wall materials of the pipe string are thinned, with low gas extraction efficiency and other challenges. Therefore, studying the flow characteristics of solid particles carried by the fluid medium at throttling tools can provide the theoretical basis for reducing the wear of throttling tools and ensuring the normal exploitation of underground coal gas [3].

At present, people have widely studied erosion wear and put forward many erosion models. Currently, the mainstream erosion prediction models are mainly as follows: DNV erosion model, E/CRC erosion model, Neilson and Gilchrist erosion model, Oka erosion model and so on. With the help of the erosion model, people have made many corresponding research results. Lin et al. [4] pointed out that the wall loss caused by particle erosion wear at the elbow is about 50 times that at the straight pipe. Solnordal et al. [5] used a Sheffield Discovery IID-8 coordinate measuring machine to draw the three-dimensional erosion data of the elbow and measured the erosion data of 38 lines along the flow direction on the inner surface of the elbow, indicating the erosion scars were all elliptical. Bikbaev et al. [6,7] found that the erosion rate increases with gas inlet velocity. Chen et al. [8] concluded that the erosion rate in the elbow is two orders of magnitude greater than that in the tee. Meng et al. [9] summarized 28 erosion prediction equations for years and listed 33 influencing parameters. Each equation contains five parameters, mainly fluid, particle properties, pipeline properties, and flow conditions. Sun Xiaoyang et al. [10] used the direct simulation Monte Carlo method to simulate and explain the mechanism of impact between particles on the erosion of gas–solid two-phase flow in the elbow. With the increase in airflow velocity, the effect between particles decreases and the erosion rate increases. Fan et al. [11] studied the new method of protecting the elbow from erosion in solid gas flow experimentally and numerically and pointed out that using fixed ribs is an effective method to reduce corrosion of the elbow in gas–solid two-phase flow. Mohammad Zamani et al. [12] studied the erosion of elbow pipes by gas-solid turbulence, showing that particle rotation greatly influences the erosion rate. Liuyun Xu et al. [15] proposed an arc-shaped diversion erosion inhibition plate structure, which can reduce the erosion rate of transitional or "V" erosion elbow by up to 41%.

All the above studies adopted the bend model to conduct erosion wear research. Since the structure's overall shape is changed only at the elbow joint in the bend model, the profile shape at the elbow is only a circular section with a specific rotation angle. Meanwhile, the geometry of the elbow profile and the overall size of the pipe column remain the same without any change. Therefore, all the above studies were only of the same size of erosion wear without changing the geometric size of the model only because of the different rotation angles of the profile. Based on the above point of view, the studies on erosion wear caused by the change in pipe string geometry have particular significance.

In this paper, based on CFD (computational fluid dynamics) and ANSYS fluent, the numerical simulation of gas–solid two-phase flow in UCG throttling tools was carried out, and the erosion wear law of throttling tools was studied by changing the geometric structure of the model and different gas velocities under the action of high temperature.

2. Overall Structural Design

2.1. Joule–Thomson Effect

The Joule–Thomson effect [14] refers to the phenomenon that the pressure of high-pressure gas will decrease and the temperature will change due to local resistance when it passes through a section with a sudden reduction in the cross-section (such as needle valve and orifice plate on the pipeline, etc.), as Figure 1 shows.

A porous plug G made of absorbent material (which can also be replaced by a capillary or needle valve) was placed in the middle of the well-insulated pipe L. When the gas with inlet pressure P_1, temperature T_1, and volume V_1 continuously passed through the porous plug G under constant pressure, it was difficult for the gas to pass through it quickly because of its sizeable blocking effect on the gas, thus maintaining a specific pressure difference between the two sides of G, making the outlet pressure drop to P_2 and the

volume change to V_2 after the gas passes through the porous plug. The outlet temperature T_2 at this time was measured. Experiments show that T_2 may be greater than, less than, or equal to T_1.

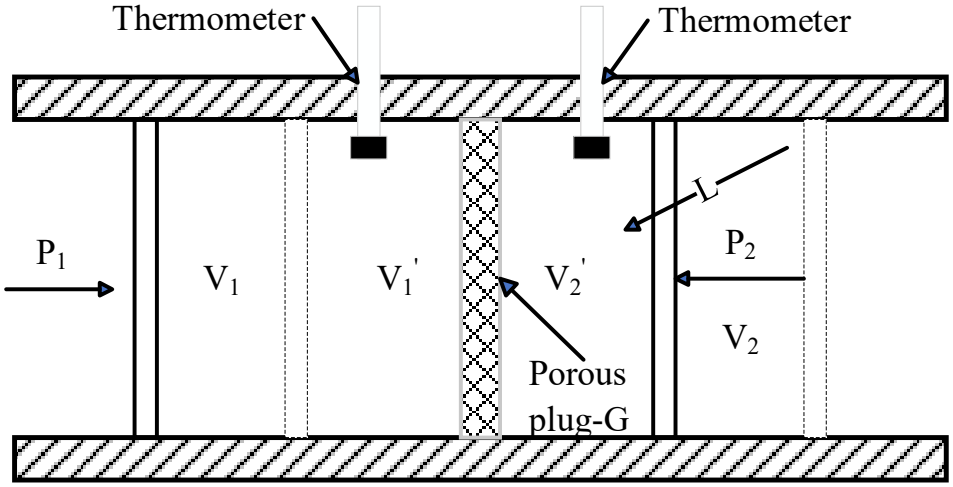

Figure 1. Schematic diagram of the Joule–Thomson effect.

2.2. Nozzle Dimension Determination

Determining the reasonable diameter of the downhole throttling nozzle is the fundamental problem of the downhole throttling and cooling effect. According to the variation law of gas flow passing through the throttle nozzle, there is the following calculation relationship between the gas well production and downhole throttle nozzle diameter when the flow state reaches the critical point [13]:

$$q_{sc} = \frac{4.066 \times 10^3 p_1 d^2}{\sqrt{\gamma_g T_1 Z_1}} \sqrt{\frac{k}{k-1}\left[\left(\frac{2}{k+1}\right)^{\frac{2}{k-1}} - \left(\frac{2}{k+1}\right)^{\frac{k+1}{k-1}}\right]} \tag{1}$$

A reasonable formula for calculating the nozzle diameter can be obtained by changing the form:

$$d = \left(\frac{1}{4.066 \times 10^3}\right)^{\frac{1}{2}} \left(\frac{q_{sc}}{p_1}\right)^{\frac{1}{2}} (\gamma_g T_1 Z_1)^{\frac{1}{4}} \left(\frac{k}{k+1}\right)^{-\frac{1}{4}} \times \left[\left(\frac{2}{k+1}\right)^{\frac{2}{k-1}} - \left(\frac{2}{k+1}\right)^{\frac{k+1}{k-1}}\right]^{-\frac{1}{4}} \tag{2}$$

In the formula q_{sc} is the gas volume flow rate, m^3/d; d is the diameter of the throttle hole, mm; k is the gas adiabatic index. Since the crude gas state is a single-phase one-dimensional flow, its range is between 1.27 and 1.3. According to experience, it is usually k = 1.29; T_1 is the temperature before throttling, K; Z_1 is the gas deviation coefficient before throttling, usually calculated as 0.9, and γ_g is the relative density of crude gas, ranging from 0.6 to 0.6034, usually 0.6034.

When designing a throttle valve, the priority is to ensure the gas well production, so the design calculation is strictly based on the given flow rate. This prevents the application of a throttle valve from achieving a strong throttling effect, which in turn affects the gas well production. According to the working conditions, the gas pressure before throttling is 30 MPa, the temperature is 800 °C, and the flow rate is 7.2×10^5 m^3/d (standard square meter) before throttling. The gas pressure is expected to drop to 10 MPa after throttling. Therefore, by substituting the above data into formula (2), it can be obtained that the theoretically calculated orifice diameter is 29.17 mm. Considering the actual manufacturing process issues, it is more appropriate to round the orifice diameter to 30 mm.

3. Mathematical Model of Erosion Simulation

3.1. Continuous Phase and Discrete Phase Models

Erosion modeling based on CFD includes three main steps: continuous phase flow field simulation, particle tracing, and erosion calculation. The gas is regarded as a constant phase and is solved by Navier–Stokes equation [16]. Particles are considered discrete phases, and Newton's second law is used to solve them. The general equations for continuity and momentum are:

$$\frac{\partial \rho}{\partial t} + \nabla(\rho \vec{u}) = 0 \tag{3}$$

$$\frac{\partial}{\partial t}(\rho \vec{u}) + \nabla(\rho \vec{u}\vec{u}) = -\nabla P + \nabla \cdot (\vec{\tau}) + \rho \vec{g} + \vec{S}_M \tag{4}$$

where ρ is the gas density; u is the instantaneous velocity vector of the gas; P is the static pressure; $\vec{\tau}$ is the stress tensor; $\rho\vec{g}$ is the volume force, and $\vec{S}_M$ is the additional momentum caused by the discrete phase.

The gas flow in the pipe string is a typical turbulent flow. By comparing CFD results with experimental data, Zhang [17] et al. found that the RNG k-ε model is the most robust turbulence model for elbow erosion. Therefore, the RNG k-ε model is used as a turbulence model in this study, and the formula is as follows:

$$\frac{\partial}{\partial t}(\rho k) + \frac{\partial}{\partial x_j}(\rho k \mu_j) = \frac{\partial}{\partial x_j}\left(\alpha_k \mu_{eff} \frac{\partial k}{\partial x_j}\right) + G_k + G_b - \rho\varepsilon \tag{5}$$

$$\frac{\partial}{\partial t}(\rho \varepsilon) + \frac{\partial}{\partial x_j}(\rho \varepsilon \mu_j) = \frac{\partial}{\partial x_j}\left(\alpha_\varepsilon \mu_{eff} \frac{\partial \varepsilon}{\partial x_j}\right) + C_{1\varepsilon}\frac{\varepsilon}{k}(G_k + C_{3\varepsilon}G_b) - C_{2\varepsilon}\rho\frac{\varepsilon^2}{k} - R_\varepsilon \tag{6}$$

where μ_{eff} is the effective viscosity; G_k, G_b is the turbulent kinetic energy, J; ε is the turbulent diffusion term; k is the turbulent kinetic energy, J; $C_{1\varepsilon} = 1.42$, $C_{2\varepsilon} = 1.68$; μ_t is the turbulent viscosity, and R_ε is an additional item.

The motion of particles in the pipe string follows Newton's second law. In the Cartesian coordinate system, the force balance equation of particles is expressed as follows [18]:

$$\frac{d\vec{u}_p}{dt} = \vec{F}_D + \vec{F}_B + \vec{F}_P + \vec{F}_{VM} \tag{7}$$

where $\vec{F}_D$ is the drag force; $\vec{F}_B$ is the buoyancy; $\vec{F}_P$ is the pressure gradient force, and $\vec{F}_{VM}$ is the additional mass force.

3.2. Erosion Model

The DNV erosion model is developed based on a large amount of experimental data and numerical prediction results, mainly used to predict the erosion of straight pipes, elbows, tee joints, welded joints, and reducers.

In the DNV erosion prediction model, the erosion rate of particles is determined by the following formula [19]:

$$E = CV_p^n f(\gamma) \tag{8}$$

$$f(\gamma) = \sum_{i=1}^{8} (-1)^{i+1} A_i \gamma^i \tag{9}$$

where n is the material correlation velocity index; C is an empirical constant; Vp is the particle impact velocity, and $f(\gamma)$ is a dimensionless function of the particle impact angle γ (in radians). For ordinary carbon steel, the value of C is 2×10^{-9} and n is 2.6. Table 1 shows the importance of the model constants in formula nine [19].

Table 1. Model constants.

A1	A2	A3	A4	A5	A6	A7	A8
9.370	42.295	110.864	110.864	170.137	98.398	31.211	31.211

3.3. Particle–Wall Interaction Behavior

In CFD software (OpenFOAM, version number v2112), the particle–wall rebound model is often combined with the erosion model to calculate the dynamic motion of particles, the erosion rate, and the maximum erosion position. Various recovery coefficients have been proposed to describe the impact of particle–wall rebound behavior. Combined with the erosion prediction model, the particles are tracked and the erosion amount is calculated. The average recovery coefficient e_n and the tangential recovery coefficient e_t represent the velocity changes after particle impact on the wall, respectively.

$$e_n = 0.988 - 0.78\theta + 0.19\theta^2 - 0.024\theta^3 + 0.027\theta^4 \quad (10)$$

$$e_t = 1 - 0.78\theta + 0.84\theta^2 - 0.21\theta^3 + 0.028\theta^4 - 0.022\theta^5 \quad (11)$$

where θ is the particle impact angle, rad, and e_n and e_t are the tangential and normal components of the wall impact recovery coefficient.

4. Numerical Simulation

4.1. Geometric Model

As Figure 2a shows, the single-hole downhole choke tool consists of five parts: the upstream pipe section, the shrinkage pipe section, the choke hole, the expanded hole pipe section, and the downstream pipe section. The double-hole downhole choke tool is similar to the single-hole structure, but the single-hole system is changed to a double-hole design, as Figure 2b shows. The overall length of the single- and double-hole downhole choke tools is 1072 mm, the diameter of the pipe string is 114.3 mm, the wall thickness of the pipe string is 9.56 mm, the hole position of the choke pipe section is designed to be located in the middle of the pipe string, the diameter of the choke hole is 30 mm, the length of the choke hole is 10 mm, the shrinkage angle at the shrinkage pipe section is 15°, and the expansion angle at the expansion pipe section is 21°. The length of the shrink hole pipe section of the single-hole throttling tool is 247 mm, and the size of the expanded hole pipe section is 175 mm, while the length of the shrink hole pipe section of the double-hole throttling tool is 95 mm, and the size of the expanded hole pipe section is 68 mm. The distance between the centers of the two throttling holes of the double-hole throttling tool is 38 mm. The materials used in the throttling devices are all carbon steel with a density of 7850. The fluid area of the geometric model is divided using the fluent meshing method, as Figure 3 shows.

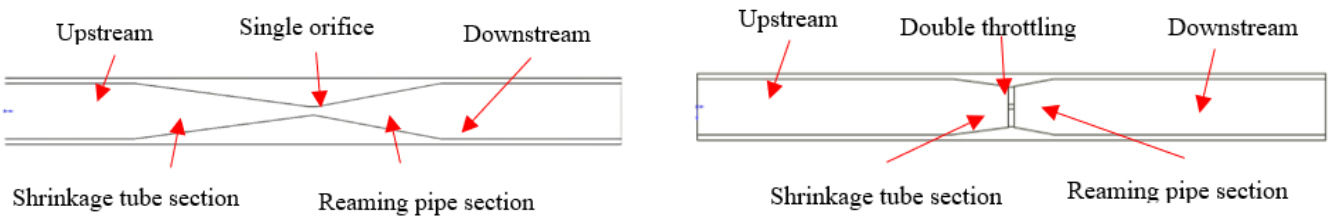

Figure 2. Geometric model of throttling tool. (**a**) Geometric model of single-hole throttling tool; (**b**) Geometric model of double-hole throttling tool.

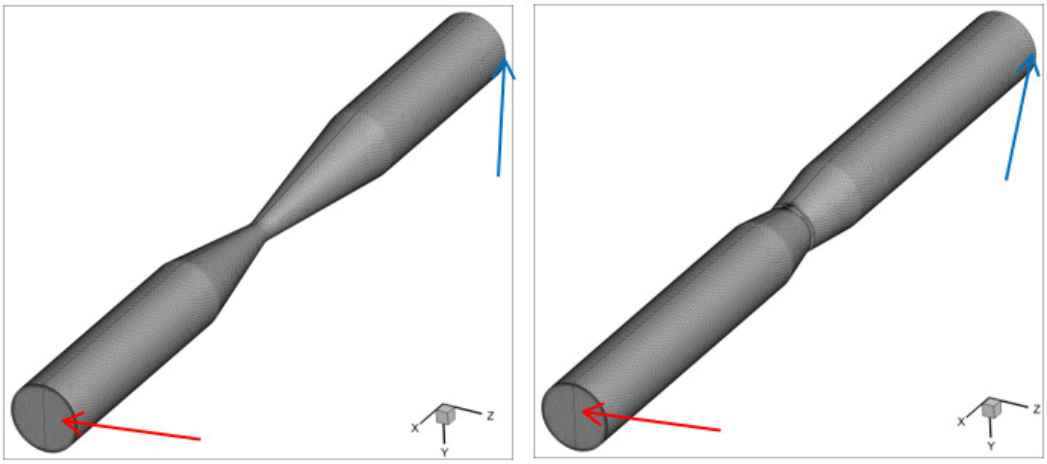

(**a**) (**b**)

Figure 3. Grid division of fluid area. (**a**) Grid division of single-hole throttling tool; (**b**) Grid division of double-hole throttling tool.

4.2. Boundary Conditions

In the erosion analysis of the throttling tool, since CH_4 accounts for a higher proportion of the gas produced during underground coal gasification, CH_4 is used as the continuous phase in the erosion analysis and its relative density is 0.6034. Because most of the underground coal is located between two rock layers, gravel is used as the discrete phase in the erosion analysis and its density is 2650. The DPM discrete phase model was used in the numerical simulation process and the particle shape was assumed to be regular spherical. As Figure 3 shows, the blue arrow indicates the inlet position of gas and pulverized coal particles and the red arrow indicates the outlet position of gas and pulverized coal particles. The inlet adopts velocity inlet; the gas velocity is 5 m/s, 10 m/s, 15 m/s, 20 m/s, and 25 m/s, respectively, and the gas temperature is 800 °C. The speed of pulverized coal particles is consistent with the direction of gas velocity. The diameter of ground coal particles is 1 mm and the mass flow rate of pulverized coal particles is 0.00011304 kg/s. The outlet adopts a pressure outlet and the outlet pressure is set to 5 MPa. Equations (10) and (11) determine the particle–wall rebound coefficient and a two-way coupling is imposed between the continuous and discrete phases.

5. Results and Analysis

5.1. Effect of Airflow Velocity on Wall Wear Distribution

The depth of erosion and wear degree of the throttling tool wall at different speeds and the distribution law of wear scars were analyzed. Figures 4 and 5, respectively, show the wall wear distribution of throttling tools with single- and double-hole structures without gas velocity. It can be seen from the figures that with the increase in gas velocity, the erosion rate of the pipe wall increases, which is mainly because the incident velocity of coal particles entering the throttling part of the pipe increases, the kinetic energy of coal particles increases, the influence effect of gravity decreases, the impact energy of particles on pipe wall is significant, and the erosion rate of the pipe string rises with the increase in gas velocity. Figure 4a demonstrates that when the gas velocity is 5 m/s, the wall wear shape of the throttling tool presents an apparent V-shaped distribution. The maximum wall wear position is at the bottom of the shrinkage cavity pipe section and most of the wall wear area is also at this position. Figure 4b demonstrates that when the gas velocity increases to 15 m/s, the wall wear shape of throttling tools is arc-shaped, and the arc-shaped opening faces the bottom of the pipe section. Currently, the maximum wall wear position is on the throttling hole surface. Most of the wall wear areas are distributed between the throttling hole and the reaming pipe section, and a small part appears at the joint between the downstream pipe section and the reaming pipe section. Figure 4c demonstrates that

when the gas velocity is 25 m/s, the wall wear shape of the throttling tool presents a spiral distribution along the wall surface of the shrinkage cavity pipe section, and the maximum wall wear position is also located on the surface of the throttling hole. Most wall wear areas appear to have jet distribution at the joint between the reaming pipe section and throttling hole, and some wall wear areas show random divergence distribution in the downstream pipe section. Figure 5 demonstrates that with the increase in speed, the maximum position of wall wear of the double-hole throttling tool shows a trend of shifting from the lower end of the joint between the shrinkage tube section and throttling hole to the upper back, and the distribution of wall wear area is mainly annular along the throttling hole wall.

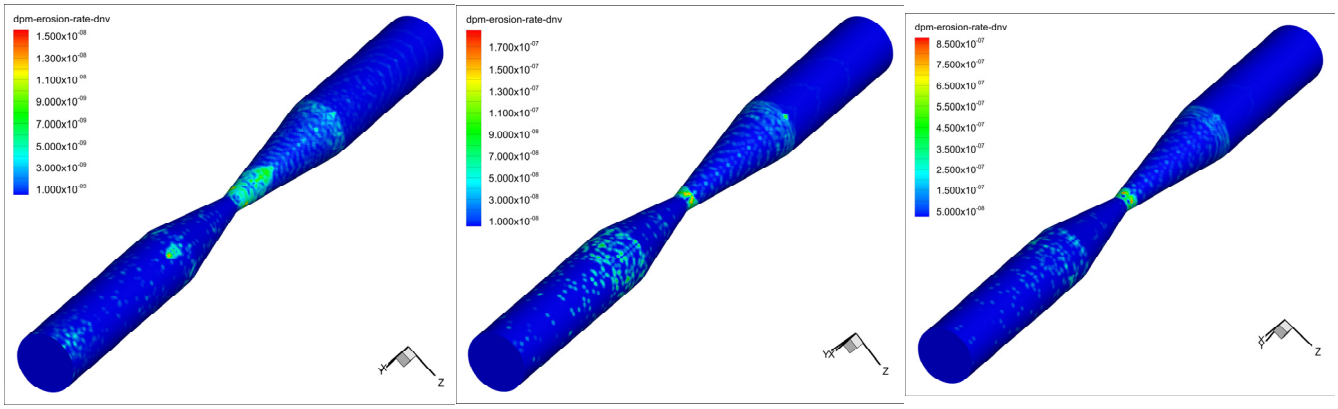

(**a**) (**b**) (**c**)

Figure 4. Wear distribution of single-orifice throttling tool wall at different gas velocities. (**a**) Wall erosion wear at gas velocity 5 m/s; (**b**) Wall erosion wear at gas velocity 15 m/s; (**c**) wall erosion wear at gas velocity of 25 m/s.

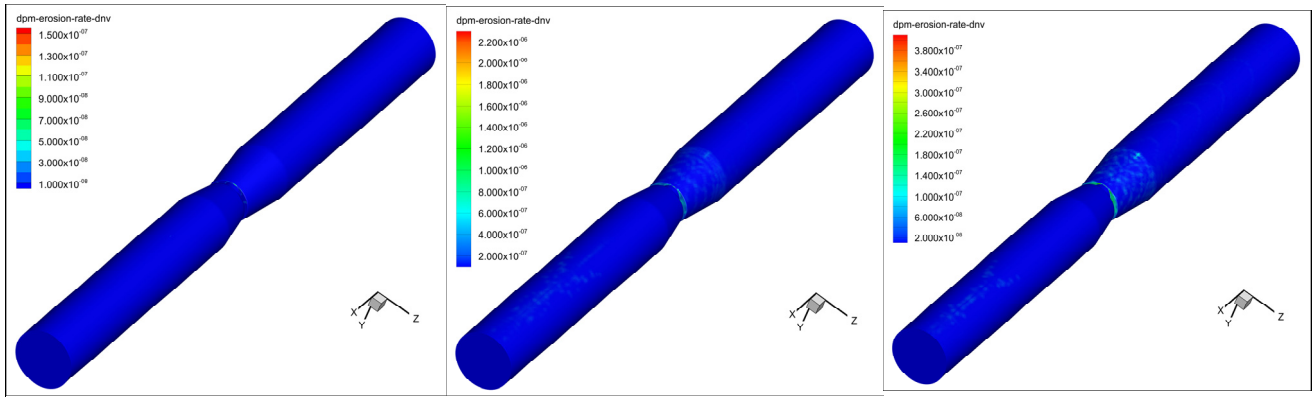

(**a**) (**b**) (**c**)

Figure 5. Wear distribution of double-hole throttling tool wall under different gas velocities. (**a**) Wall erosion wear at gas velocity of 5 m/s; (**b**) Wall erosion wear at gas velocity of 15 m/s; (**b**) Wall erosion wear at gas velocity of 25 m/s.

The main reasons for the different distribution of the two wall wear areas are as follows: the single-hole throttling tool adopts the through-hole design. It will not produce a wall at the throttling hole, thus ensuring that the gas and solid particles will not create obstacles in the transportation process and avoiding energy loss. However, the double-hole throttling tool adopts a double-hole design to produce an annular wall in the throttling hole, which will hinder the transportation process of gas and solid particles to a certain extent and cause energy loss, leading to the difference in wall wear area distribution between them.

5.2. Influence of Airflow Velocity on Wall Impact Position

Because of the incident angle of particles, when the gas flows horizontally with the pipe wall, Figure 6a demonstrates that when the gas velocity is 5 m/s, because of the action of inertia, fluid drag force, and gravity, a large number of particles collide with the wall surface of the shrinkage tube section at the junction of the shrinkage tube section and the upstream tube section for the first time. After the first collision, some pulverized coal particles rebounded from the wall surface along the shrinkage cavity direction of the lower end of the shrinkage tube section and collided with the upper end of the throttling orifice for the second time. At this time, most of the particles still wear severely with the lower surface of the throttling orifice because of their small kinetic energy, so the maximum wear area of the wall surface is located on the lower surface of the throttling orifice. Meanwhile, the kinetic energy of the pulverized coal particles causes damage. Figure 6b,c demonstrate that when the gas velocity increases, the pulverized coal particles will not affect the movement process of the particles with the gas because of their inertia, fluid drag force, and gravity. The structural design of the pipe string is the main factor affecting the movement process of pulverized coal particles. In the shrinkage cavity section, the peripheral particles will collide with the inner surface of the shrinkage cavity section for the first time. Still, the overall movement form of the pulverized coal particles will not change. When the ground coal particles flow through the reaming section, the ground coal particles will diffuse due to the increase in the spatial volume of the pipe string. In contrast, the peripheral pulverized coal particles will collide with the reaming section for the second time. In contrast, the spatial volume of the reaming area will increase gradually, so it will not affect the inner surface of the flow hole.

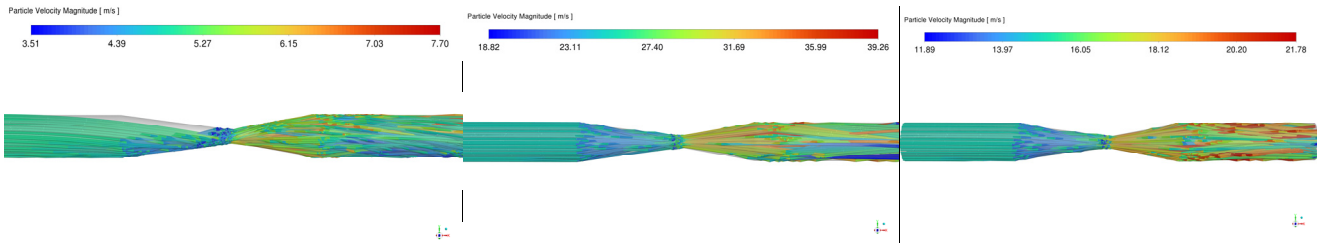

(**a**) (**b**) (**c**)

Figure 6. Particle trajectory distribution in the flow field of single-orifice throttling tool at different gas velocities. (**a**) Particle trajectory distribution with gas velocity of 5 m/s; (**b**) Particle trajectory distribution at gas velocity of 15 m/s; (**c**) Particle trajectory distribution at gas velocity of 25 m/s.

Figure 7a demonstrates that when the gas velocity is 5 m/s, a large number of particles collide for the first time at the joint between the lower orifice and the shrinkage tube section due to their inertia, fluid drag force, and gravity, and form annular erosion scars distributed along the orifice. At this time, after the second collision between the ring wall and some pulverized coal particles at the orifice, the particle rebound occurs, and the clash between particles is not apparent. Most particles collide for the third time with the wall of the downstream tube section when the gas velocity is 15 m/s and the collision position is far away from the reaming tube section. Figure 7b demonstrates that when the gas velocity is 15 m/s, most of the particles still flow through the lower orifice of the tube string and the first collision occurs at the joint. However, due to the fewer particles flowing through the upper orifice, the maximum wall erosion rate still occurs at the joint between the lower orifice and the shrinkage cavity pipe section, and the annular erosion distribution along the lower end of the throttle pipe section intensifies and tends to shift upward. More pulverized coal particles collide with the annular wall produced by the structural design for the second time and the particle backflow phenomenon intensifies. The position of the third collision of particles is close to the outlet of the downstream pipe section. Collisions between particles are not very obvious. Figure 7c demonstrates that the number of particles

flowing through the upper and lower orifices are roughly the same when the gas velocity is 25 m/s. In contrast, the particle rebound phenomenon occurs due to the first collision between the particles and the annular wall produced by the structural design. Because the kinetic energy of pulverized coal particles following the gas flow is more significant at this time, the kinetic energy decreases sharply after collision with the annular wall. The kinetic energy increases along the negative direction of gas flow and the subsequent particles along the gas velocity direction collide, aggravating the collision phenomenon between particles and causing a certain degree of energy loss, so the erosion rate of the lower orifice decreases. After the collision between particles, the number of pulverized coal particles flowing through the upper orifice in a unit of time is reduced compared with the number of ground coal particles flowing through the lower orifice due to the self-weight of pulverized coal particles, so the maximum wall wear position is still at the joint between the lower orifice and the shrinkage cavity pipe section. The second collision occurs between the pulverized coal particles in the reaming pipe section and the downstream pipe section, and the third collision occurs near the outlet of the downstream pipe section.

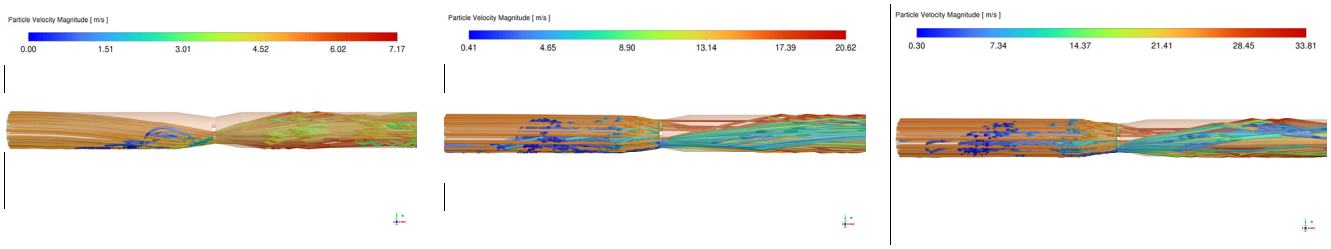

(**a**) (**b**) (**c**)

Figure 7. Particle trajectory distribution of internal flow field of double-hole throttling tool under different gas velocities. (**a**) Particle trajectory distribution with gas velocity of 5 m/s; (**b**) Particle trajectory distribution at gas velocity of 15 m/s; (**c**) Particle trajectory distribution at a gas velocity of 25 m/s.

Because of the structural differences of throttling tools, the pulverized coal particles show different trajectory characteristics in the movement process, so the different positions of wall wear areas, the collision times between ground coal particles and wall, and the maximum wall wear rate are all within the reasonable discussion range of structural differences.

5.3. Influence of Airflow Velocity on Wall Erosion Effect

Classic prediction methods are based on regression and statistical analysis theories (regression, autoregressive models); probabilistic and modern prediction methods use traditional and deep machine learning algorithms, rank analysis methods, fuzzy set theory, singular spectrum analysis, wavelet transform, gray models, etc. Figure 8 shows the statistical analysis of the wall erosion rate in origin and demonstrates that when the gas velocity is 5–25 m/s, the wall wear rate of the single-hole throttling tool is positively correlated with the gas velocity and the curve growth rate gradually increases. The wall wear rate increases with gas velocity and all pulverized coal particles flow into and out of the throttle inlet. When the gas velocity is 5–20 m/s, the wall wear rate of the double-orifice throttling tool is positively correlated with the gas velocity and the curve growth rate increases gradually—the wall wear rate increases with the increase in the gas velocity. Because of the inertia and gravity of the pulverized coal particles, most of the particles flow through the lower orifice of the double-orifice throttling tool. However, when the gas velocity is 25 m/s, the wall wear rate of the double-orifice throttling device is negatively correlated with the gas velocity and the curve growth rate decreases or grows slowly. The main reason for this phenomenon is that the number of pulverized coal particles flowing through the upper orifice gradually increases under the influence of inertia and gravity, and the number of particles flowing through the lower orifice decreases per unit time with the increase in gas velocity, so the erosion rate at the lower end of the orifice decreases.

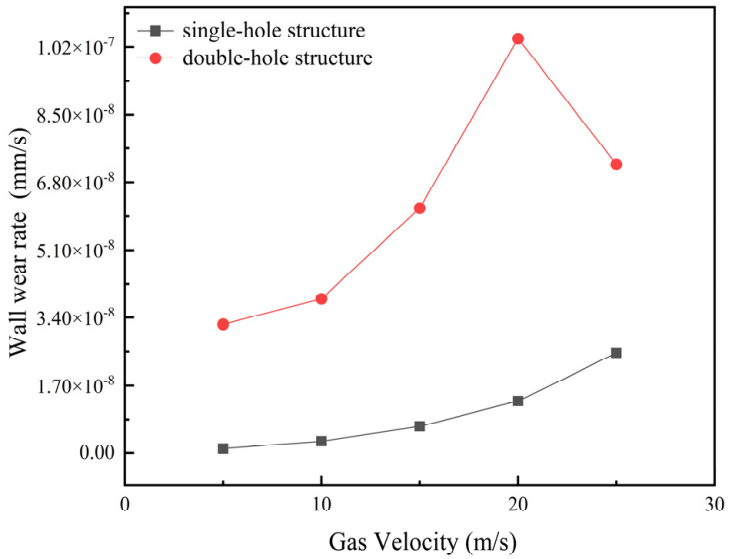

Figure 8. Erosion wear statistics of throttling tools under different gas velocities.

Generally speaking, under the same working conditions, in the process of UCG, the wear degree of unburned pulverized coal particles trapped by underground high temperature and high-pressure gas is obviously better than that of the double-hole structure and the overall wall wear rate is lower. The main reason for this phenomenon is that the single-hole system adopts a through-hole design, and the length of the shrinkage cavity pipe section and reaming pipe section is longer than that of the double-hole structure, which avoids the phenomenon of a sudden change in geometry shape and excessive deformation in the pipe wall. At the same time, the double-hole facility will produce an annular wall at the throttling hole in design, which hinders the movement of gas and pulverized coal particles to a certain extent, resulting in a large number of ground coal particles colliding with the annular wall for many times in a short time.

6. Conclusions

Aiming at the downhole throttling tools with different structures, the erosion prediction model of downhole throttling tools with two-way coupling of gas–solid two-phase flow is established in this paper and the erosion of downhole throttling tools under actual working conditions is calculated. The difference in wall wear distribution, wall collision position, and wall erosion effect of throttling tools with different structures is studied with the change in gas velocity. Based on the above results, the following conclusions are drawn:

(1) When the gas velocity ranges from 5 to 25 m/s, there are three kinds of distribution of wall wear area in the single-hole throttling tool: V-shaped distribution with a gas velocity of 5 m/s, arc-shaped distribution with a gas velocity of 15 m/s, and spiral distribution along the wall of the shrinkage tube with a gas velocity of 25 m/s. The distribution positions of the three shapes are all at the joint between the shrinkage cavity pipe section and the upstream pipe section. In the gas velocity range of 5–25 m/s, there is only one type of wall wear area distribution: annular distribution from bottom to top along the annular wall.

(2) When the gas velocity of a single-orifice throttle is 5 m/s, pulverized coal particles collide with the wall of the pipe string three times, and the collision positions are the joint between the shrinkage pipe section and upstream pipe section, the upper end of the throttling orifice inlet, and the lower wall of the downstream pipe section. When the gas velocity is more than 5 m/s, the two collisions between pulverized coal particles and the wall of the pipe string occur in the shrinkage pipe section and the reaming pipe section. When the gas velocity ranges from 5 to 25 m/s, the pulverized coal particles collide thrice with the pipe string wall. However, when the gas velocity

is 5 m/s, the ground coal particles flow through the lower orifice and hit the joint of the lower orifice and the shrinkage pipe section, the annular wall produced by the double-orifice structure, and the upper and lower walls of the downstream pipe section. When the gas velocity is more significant than 5 m/s, the upper and lower orifices have pulverized coal particles flowing through and the collision position is the joint of the orifice and shrinkage cavity pipe section. The annular wall produced by the double-hole structure is the upper surface of the downstream pipe section.

(3) Single-hole structures adopt through-hole and progressive expansion, and contraction pipe section designs avoid sudden changes in geometric shape and excessive and rapid deformation of the pipe wall in double-hole structures. It avoids the generation of the annular wall in a double-hole design. Under the same working conditions, the wall wear rate of a single-hole design is less than that of a double-hole design, so the erosion wear resistance of a single-hole system is better than that of a double-hole design.

7. Discussion

(1) Whether the different distribution of wall erosion and wear rate is related to the shrinkage angle and expansion angle of the throttle hole.
(2) Whether the numerical value of the erosion and wear rate on the pipe string wall is correlated with the particle diameter and particle mass flow rate.
(3) Whether the location of erosion and wear on the pipe string wall is correlated with the diameter, length, and number of the orifices.

Author Contributions: Conceptualization, J.W.; methodology, B.Z.; software, J.F.; validation, S.Y. and B.Z.; formal analysis, J.W.; investigation, C.W.; resources, X.R.; writing—original draft preparation, B.Z. All authors have read and agreed to the published version of the manuscript.

Funding: This research is supported by National Key R&D Program of China (2023YFC3009205) and CNPC Basic Research Project (2023Z11, 2021DQ03 (2022Z-03)).

Data Availability Statement: No new data were created or analyzed in this study.

Conflicts of Interest: Author Wang Jianjun was employed by CNPC Tubular Goods Research Institute. Authors Fu Jianglong and Wang Chao were employed by The Second Gas Plant of PetroChina Changqing Oilfield Company, Tubular Goods Research Institute. Author Ren Xiangyi was employed by CNPC Tubular Goods Research Institute. The remaining authors declare that the research was conducted in the absence of any commercial or financial relationships that could be construed as potential conflicts of interest.

References

1. Mandal, R.; Maity, T. Operational process parameters of underground coal gasification technique and its control. *J. Process Control.* **2023**, *129*, 103031. [CrossRef]
2. Lin, N.; Lan, H.; Xu, Y.; Dong, S.; Barber, G. Effect of the gas–solid two-phase flow velocity on elbow erosion. *J. Nat. Gas Sci. Eng.* **2015**, *26*, 581–586. [CrossRef]
3. Peng, W.; Cao, X. Numerical prediction of erosion distributions and solid particle trajectories in elbows for gas–reliable flow. *J. Nat. Gas Sci. Eng.* **2016**, *30*, 455–470. [CrossRef]
4. Malozyomov, B.V.; Golik, V.I.; Brigida, V.; Kukartsev, V.V.; Tynchenko, Y.A.; Boyko, A.A.; Tynchenko, S.V. Substantiation of Drilling Parameters for Undermined Drainage Boreholes for Increasing Methane Production from Unconventional Coal-Gas Collectors. *Energies* **2023**, *16*, 4276. [CrossRef]
5. Solnordal, C.B.; Wong, C.Y.; Boulanger, J. An experimental and numerical analysis of erosion caused by sand pneumatically conveyed through a standard pipe elbow. *Wear* **2015**, *336–337*, 43–57. [CrossRef]
6. Bikbaev, F.A.; Maksimenko, M.Z.; Berezin, V.L.; Krasnov, V.I.; Zhilinskii, I.B. Wear on branches in pneumatic conveying ducting. *Chem. Pet. Eng.* **1972**, *8*, 465–466. [CrossRef]
7. Bikbaev, F.A.; Krasnov, V.I.; Maksimenko, M.Z.; Krasnov, V.I.; Zhilinskii, I.B. Leading factors affecting gas abrasive wear of elbows in pneumatic conveying pipes. *Chem. Pet. Eng.* **1973**, *9*, 73–75. [CrossRef]
8. Chen, X.; Mclaury, B.S.; Shirazi, S.A. Numerical and experimental investigation of the relative erosion severity between plugged tees and elbows in dilute gas/solid two-phase flow. *Wear* **2006**, *261*, 715–729. [CrossRef]
9. Meng, H.C.; Ludema, K.C. Wear models and predictive equations: Their form and content. *Wear* **1995**, *181–183*, 443–457. [CrossRef]

10. Sun, X.Y.; Cao, X.W.; Xie, Z.Q.; Fu, C.Y. Erosion prediction of gas-solid two-phase flow based on DSMC-CFD method. *Surf. Technol.* **2020**, *49*, 274–280.
11. Fan, J.; Yao, J.; Zhang, X.; Cen, K. Experimental and numerical investigation of a new method for protecting bends from erosion in gas-particle flows. *Wear* **2001**, *251*, 853–860. [CrossRef]
12. Zamani, M.; Seddighi, S.; Nazif, H.R. Erosion of natural gas elbows due to rotating particles in turbulent gas-solid flow. *J. Nat. Gas Sci. Eng.* **2017**, *40*, 91–113. [CrossRef]
13. Xu, L.; Wu, F.; Yan, Y.; Ma, X.; Hui, Z.; Wei, L. Numerical simulation of air-solid erosion in the elbow with novel arc-shaped diversion erosion-inhibiting plate structure. *Powder Technol.* **2021**, *393*, 670–680. [CrossRef]
14. Cheng, Y. *Study on Joule-Thomson Effect of the Micro-Flow Field in Aerostatic Throttle*; China Jiliang University: Hangzhou, China, 2016.
15. Zhou, Y.M.; Huang, W.M.; Huang, D.Y. Computation of Gas Well Choke and Discussions on Its Routinization. *Inn. Mong. Petrochem.* **2021**, *47*, 54–58.
16. Yakhot, V.; Orszag, S.A. Renormalization group analysis of turbulence I. Basic theory. *J. Sci. Comput.* **1986**, *57*, 3–51. [CrossRef]
17. Zhang, J.; Mclaury, B.S.; Shirazi, S.A. Application and experimental validation of a CFD-based erosion prediction procedure for jet impingement geometry. *Wear* **2018**, *394–395*, 11–19. [CrossRef]
18. Parsi, M.; Najmi, K.; Najafifard, F.; Hassani, S.; McLaury, B.S.; Shirazi, S.A. A comprehensive review of solid particle erosion modeling for oil and gas wells and pipelines applications. *J. Nat. Gas Sci. Eng.* **2014**, *21*, 850–873. [CrossRef]
19. Forder, A.; Thew, M.; Harrison, D. A numerical investigation of solid particle erosion experienced within oilfield control valves. *Wear* **1998**, *216*, 184–193. [CrossRef]